ADVANCED OPTICAL MATERIALS
www.advopticalmat.de

The Impact of Donor-Orientation on the Emission Properties of Chlorinated Trityl Radicals

Mona E. Arnold, Robert Toews, Lars Schneider, Jonas Schmid, Miftahussurur Hamidi Putra, Michael Busch, Axel Groß, Felix Deschler,* Andreas Köhn,* and Alexander J. C. Kuehne**

Chlorinated trityl radicals functionalized with electron-donating groups are promising red-emitting materials for optoelectronic and spintronic applications, overcoming the spin-statistical limit of conventional emitters. Donor functionalization induces charge transfer character, enhancing photoluminescence quantum yield, which depends on the donor strength and its orientation. However, donor-functionalized tris(trichlorophenyl)methyl radicals often show lower quantum yield than their perchlorinated derivatives, likely due to weaker donor-acceptor electronic coupling and enhanced non-radiative decay. A novel trityl derivative is presented with two additional chlorines that restrict the orientation of the donor to a nearly perpendicular arrangement toward the trityl plane, minimizing vibronic coupling and non-radiative losses. Spectroscopic and computational studies reveal that this steric constraint improves the photoluminescence quantum yield compared to the tris(trichlorophenyl)methyl analogs. These findings highlight the potential of donor-acceptor decoupling to enable efficient, redshifted emission, offering a design strategy for high-performance radical emitters.

1. Introduction

Stable, chlorinated trityl radicals functionalized with electron-donating units represent promising candidates as efficient red emitters for organic light-emitting diodes. Since states of higher multiplicity appear only at higher energies in radical emitters, the emission occurs from doublet states upon electrical excitation, and the spin-statistical limitation of conventional emitters to 25% internal quantum efficiency is lifted.[1–6] Typically, chlorinated trityl radicals exhibit only low photoluminescence quantum yield ϕ_{PL}, because the relevant transitions are symmetry-forbidden. However, the emission performance can be improved by appropriate functionalization with electron-donating groups, evoking symmetry breaking and a charge transfer (CT) excited state.[7–11] Both, the emission wavelengths λ_{max} and ϕ_{PL} highly depend on the electron-donating strength of the substituent.[12] Moreover, the structural arrangement of the donor relative to the trityl radical appears to have a significant impact on the emission characteristics, exemplified by the comparison of trityl radical functionalized with triphenylamine (TPA), 3-phenylcarbazole (3PCz) and phenyl-*N*-carbazole (PCz). Interestingly, the three donors all exhibit a triphenylamine scaffold, in which a bond between two phenyl rings evokes a planarized carbazole unit

M. E. Arnold, J. Schmid, A. J. C. Kuehne
Institute of Organic and Macromolecular Chemistry
Ulm University
Albert-Einstein-Allee 11, 89081 Ulm, Germany
E-mail: mona.arnold@uni-ulm.de; alexander.kuehne@uni-ulm.de

R. Toews, A. Köhn
Institute for Theoretical Chemistry
University of Stuttgart
Pfaffenwaldring 55, 70569 Stuttgart, Germany
E-mail: koehn@theochem.uni-stuttgart.de

L. Schneider, F. Deschler
Institute for Physical Chemistry
Heidelberg University
Im Neuenheimer Feld 229, 69120 Heidelberg, Germany
E-mail: felix.deschler@pci.uni-heidelberg.de

M. H. Putra, A. Groß
Institute of Theoretical Chemistry
Ulm University
Oberberghof 7, 89069 Ulm, Germany

M. Busch
Division of Materials Science
Department of Engineering Sciences and Mathematics
Luleå University of Technology
971 87 Luleå, Sweden

M. Busch
Wallenberg Initiative Materials Science for Sustainability (WISE)
Luleå University of Technology
971 87 Luleå, Sweden

A. Groß
Helmholtz Institute Ulm (HIU) for Electrochemical Energy Storage
Helmholtzstraße 11, 89081 Ulm, Germany

The ORCID identification number(s) for the author(s) of this article can be found under https://doi.org/10.1002/adom.202500296

DOI: 10.1002/adom.202500296

in the case of the 3PCz and PCz units. This planarization leads to significant differences in the trityl emission efficiency. More interestingly, when attaching the same donor to the tris(trichlorophenyl)methyl radical (TTM) or the perchlorinated trityl radical (PTM), the TTM analogs exhibit lower ϕ_{PL} than the PTM derivatives, while the underlying reasons have not been elucidated yet.[1,13,14] The obvious difference between the TTM and PTM derivatives is the disparate acceptor strength induced by the higher number of chlorine substituents in the PTM. Moreover, the added chlorine substituents in PTM may restrict the rotation and the orientation of the donor toward the trityl radical plane. The suppression of geometric differences in the ground and excited state favors efficient emission by minimizing non-radiative relaxation.[15,16] A smaller dihedral angle between the donor and the trityl plane ($\measuredangle_{DA}$) has been suggested to lead to enhanced electronic coupling between the donor and the trityl orbitals, leading to more efficient emission.[13] However, this is in contrast to the experimentally observed ϕ_{PL} of donor-functionalized TTM radicals, which are much dimmer compared to the PTM homologues. Steric effects have been investigated for two- and three-fold aryl-substituted trityl radicals.[9,10,17] Functionalization with mesityl boosts the quantum yield through a combination of symmetry-breaking CT and reduced internal conversion, due to steric hindrance.[17] So far, adjusting the extent of steric hindrance between trityl and donor is typically achieved by modification of the donor site.[10,17]

A recent report has shown that high ϕ_{PL} in donor functionalized TTM radicals can be explained by the absence of high-frequency vibrations, for example, carbon–carbon stretching modes that could couple to the first excited doublet state (D_1) and lead to its non-radiative relaxation.[18] In trityl radicals, the D_1 is typically described as a charge transfer (CT) state.[7,15,19,20] The higher the frequency of the vibration coupling to the CT exciton, the more likely becomes vibrational deactivation, leading to high non-radiative recombination rates. In donor-functionalized trityl radicals, higher-lying excited states (D_2 and above) are accessible by excitation in the blue and UV spectral region. These higher excited states exhibit significant locally excited (LE) state character and can accommodate strong couplings to high-frequency vibrations.[18] While higher excited states in donor-functionalized trityl radicals typically relax quickly to the D_1 state, coupling to high-frequency vibrations occurs on timescales that can compete with internal conversion. Therefore, such vibronic effects in higher excited states could contribute to non-radiative relaxation. If the LE character in light-emitting trityl radicals could be reduced, to avoid coupling to high-frequency modes located on the trityl site, then, it would be possible to further improve the emission characteristics of donor-functionalized trityl radicals. Electronic decoupling of the donor and acceptor moieties has been demonstrated to suppress non-radiative relaxation in a series of donor-functionalized PTM radicals.[20] This concept would also allow to overcome the restrictions of the energy gap law and achieve high ϕ_{PL} for emission that is strongly redshifted into the near IR spectrum. However, to date, there is no study that independently investigates the effect of steric restriction of the donor rotation to produce clear CT excited states on the emission performance.

Here, we introduce a new trityl derivative (TBTM) carrying only two additional chlorine atoms on the phenyl ring connected to the donor, to systematically study the impact of donor orientation without significantly changing the electronic properties and acceptor strength of the trityl radical moiety. Employing identical substituents for TTM and TBTM allows for direct comparison and a systematic investigation of steric effects without altering the electronic properties of the donors. While the electron-accepting strength of the radical moiety is only slightly modified compared to TTM, we show that the additional chlorines restrict the orientation of the donor to almost perpendicular with respect to the TBTM plane. We employ spectroscopy and quantum chemical calculations to explain the improved emission characteristics of the TBTM compared to the TTM derivatives, enabling the rational design of future high-performance radical emitters.

2. Results and Discussion

2.1. Synthesis

We start by preparing the new unsymmetrically chlorinated TBTM (4-bromo-2,3,5,6-tetrachlorophenyl)bis(2,4,6-trichlorophenyl)methyl radical. First, 3-bromo-1,2,4,5-tetrachlorobenzene is alkylated using chloroform to give the halogenated benzyl derivative **2**. The latter is then used in a subsequent Friedel-Crafts alkylation to give the unsymmetrically chlorinated triphenyl methane **1** in excellent overall yield. The *para*-bromide functionality allows efficient Suzuki cross-coupling of the respective electron donors (PCz, 3PCz, TPA).

Fortunately, the steric hindrance caused by the chlorine atoms in the *meta*-position does not lower the reactivity of the bromide site in **1**, allowing donor functionalization in good to excellent yields at mild conditions (see **Figure 1**). The corresponding donor-functionalized TBTM radicals are obtained following the established deprotonation-oxidation protocol.[7,13,21,22] Deprotonation of the α-carbon using potassium *tert*-butoxide is followed by mild oxidation of the carbanion to the radical using *p*-chloranil. The open-shell nature of the resulting compounds is confirmed by electron paramagnetic resonance (EPR) spectroscopy (see Figure S2, Supporting Information).

Additionally, we synthesize the TTM series carrying the respective donors for direct comparison (see Figure 1). For this series of TTM-TPA, TTM-3PCz, and TTM-PCz radicals, we develop slightly adapted reaction procedures inspired by synthetic protocols from the literature.[13,14] In contrast to previously reported procedures starting from HTTM,[21] our method delivers improved yields of 49% for TTM-TPA, 80% for TTM-3PCz, and 93% for TTM-PCz (see the Supporting Information for experimental details).[13,18]

We perform cyclic voltammetry measurements for the radicals and observe the reduction of the TBTM moieties to be shifted by ≈0.1 V toward higher potentials compared to TTM (see Figure S24, Supporting Information). This indicates that the additional chlorine atoms render the TBTM trityl site a slightly stronger electron acceptor.

2.2. Analysis of the Excited State Characteristics

We characterize our donor-functionalized radicals using UV–vis spectroscopy. To avoid strong interactions of the radicals in the

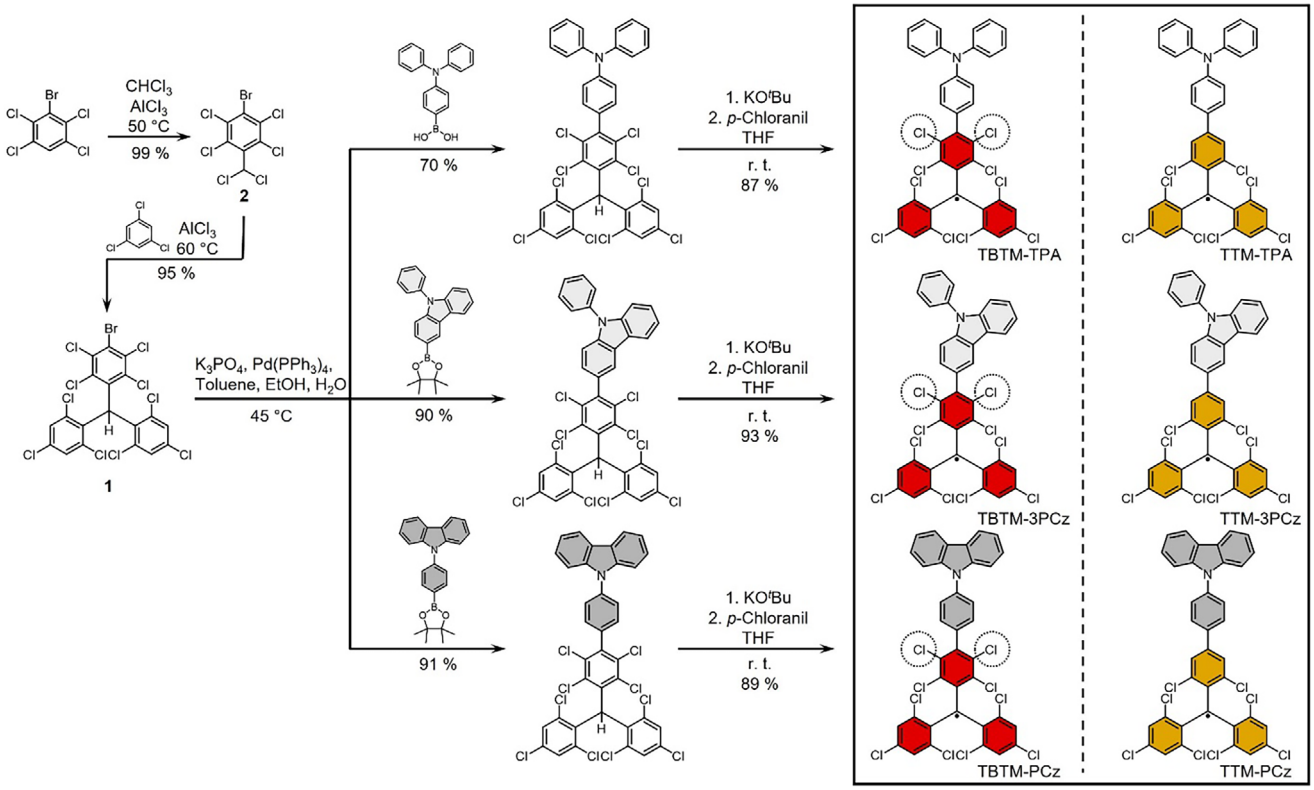

Figure 1. Synthesis of new donor-functionalized TBTM trityl radicals carrying eight chlorine atoms. The unsymmetric precursor for Suzuki coupling 1 is obtained from a two-step Friedel-Crafts alkylation reaction. TTM derivatives with identical donors are shown for comparison.

excited state with the solvent, we choose cyclohexane as a suitable non-polar solvent. When we compare the UV–vis absorption spectra of our TBTM and TTM derivatives, we observe characteristic features of trityl radicals, including strong absorption in the UV and a weak band in the visible region, typically associated with the $D_0 \rightarrow D_1$ transition (see **Figure 2**). The strong absorption in the UV is insensitive to the donor substitution, substantiating the LE character of the higher-energy transition (see Figure 2). By contrast, the $D_0 \rightarrow D_1$ absorption at lower energy undergoes a red-shift from PCz to 3PCz and TPA, correlating with the donor strength and indicating the increasing CT character of the transition with increasing donor strength (see Figure 2 and **Table 1**). This order of the donor strength is consistent with the oxidation potentials observed in the voltammograms (see Figure S24, Supporting Information). Moreover, the observation of a bathochromic shift with increasing donor strength is in agreement with prior reports for donor-functionalized TTM and PTM derivatives.[12,20] The shift can be rationalized by an increased stabilization, as the CT character of the excited state becomes more pronounced. Notably, the extinction coefficients ϵ for the $D_0 \rightarrow D_1$ transition are reduced in the TBTM series with respect to the TTM series (see Figure 2 and Table 1). This

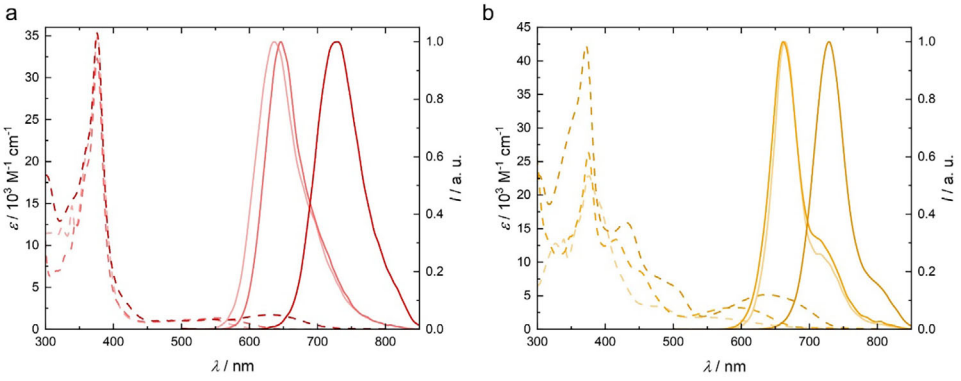

Figure 2. Absorption (dashed lines) and emission (solid lines) spectra measured for cyclohexane solutions (10^{-4} M) of a) TBTM (red) and b) TTM (orange), functionalized with TPA (dark color), 3PCz (medium color), and PCz (light color).

Table 1. Measured photophysical properties for cyclohexane solutions of TBTM and TTM, functionalized with identical substituents, along with computed (DFT/TD-DFT) dihedral angles $\measuredangle_{DA}$ between donor and trityl moieties of the radicals in their ground and excited state geometry, and norms of the nonadiabatic coupling vectors $|D^{(01)}|$ for the D_0 and D_1 state and $|D^{(12)}|$ for the D_1 and D_2 state.

Compound	λ_{abs}/nm	ϵ (D_0-D_1) / 10^3 M^{-1} cm^{-1}	λ_{em}/nm	ϕ_{PL}/%	τ/ns	$k_r/10^6$ s^{-1}	$k_{nr}/10^6$ s^{-1}	$\measuredangle_{DA}$ (GS)/°	$\measuredangle_{DA}$ (ES)/°	$\lvert D^{(01)}\rvert$/cm^{-1}	$\lvert D^{(12)}\rvert$/cm^{-1}
TBTM-TPA	630	1.73	729	43	17.1	25.1	33.3	70	65	29	76
TBTM-3PCz	548	1.37	646	59	27.3	21.6	15.0	72	53	45	568
TBTM-PCz	543	1.15	636	16	12.7	12.6	66.1	90	90	6	76
TTM-TPA	635	5.14	729	12	6.4	18.8	137.5	31	12	70	116
TTM-3PCz	593	3.25[a)]	664	27	15.7	17.2	46.5	32	13	80	283
TTM-PCz	545	1.82[a)]	662	4	4.6	8.7	208.7	33	8	71	330

[a)] Values adopted from ref. [13].

reduction in ϵ indicates diminished electronic coupling between donor and trityl units in the donor-functionalized TBTM radicals compared to the TTM series. Presumably, a larger dihedral angle ($\measuredangle_{DA}$) between donor and trityl radical in the TBTM series, due to the steric constraints of the *meta*-chlorides (*ortho* to the donor moieties), could be the reason for the weakened electronic coupling.

To gain further insight into the geometry and the transitions of the donor functionalized TBTM and TTM radical series, we perform time-dependent density functional theory (TD-DFT) calculations using a modified CAM-B3LYP functional[23] (γ = 0.098 a_0^{-1}) and def2-SVP basis sets (see SI for computational details).[24] We optimize the molecules in their ground state geometry to determine $\measuredangle_{DA}$(GS). As expected, we find large dihedral angles $\measuredangle_{DA}$(GS) = 70°–90° for the TBTM series, while the TTM derived radicals show significantly smaller $\measuredangle_{DA}$(GS) = 31°–33° (see **Figure 3a** and Table 1). Apparently, the additional *meta*-chloride groups in TBTM induce indeed sufficient steric hindrance to enforce a much larger dihedral angle between donor and acceptor compared to TTM.

We also compute the excited state (D_1) geometry on the CAM-B3LYP ($\gamma = 0.098\ a_0^{-1}$), def2-SVP level, and we find that the donor substituents tend to rotate into the trityl plane upon excitation. For the TBTM series, the change in dihedral angle is typically smaller than for the TTM series. In addition, the resulting dihedral angles in the excited state are larger for the TBTM ($\measuredangle_{DA}$(ES) = 53–90°) than for the TTM ($\measuredangle_{DA}$(ES) = 8–13°) derivatives (cf. Table 1).

We calculate the natural transition orbitals (NTOs) for the $D_0 \rightarrow D_1$ transition to learn whether the transition has more LE or CT character (see Figure 3b,c). For all molecules under investigation, the electron NTO is located on the trityl moiety, whereas

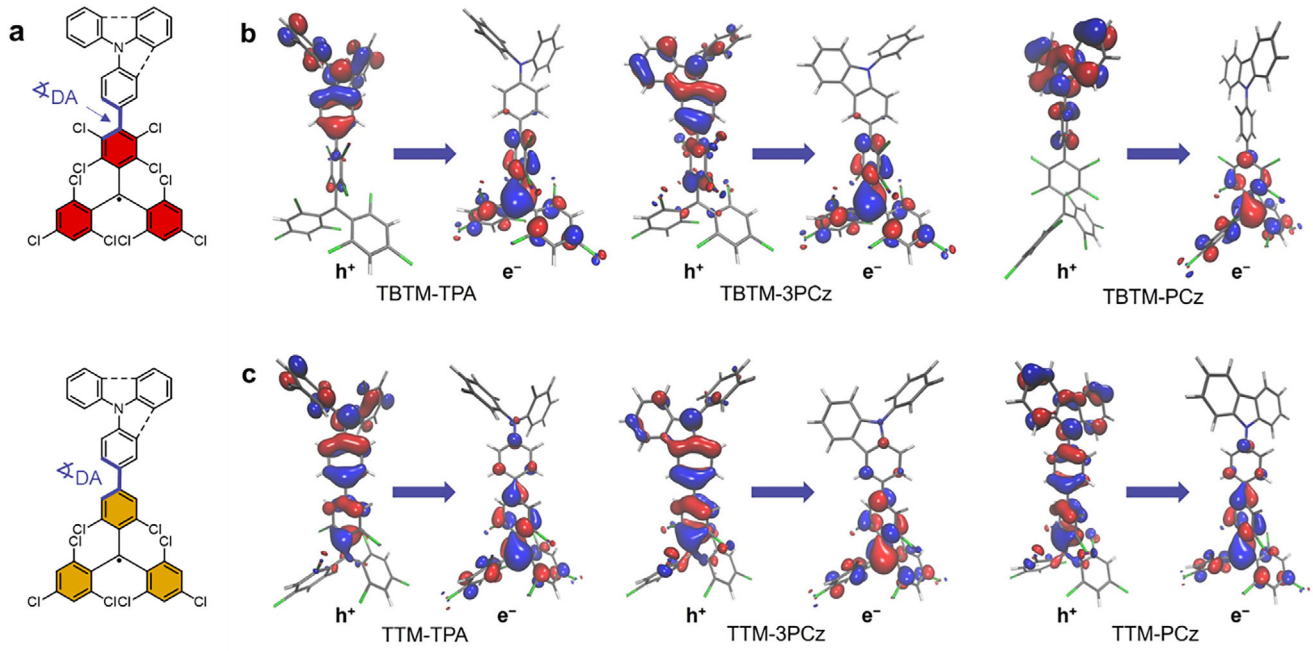

Figure 3. a) Chemical structure of TTM and TBTM derivatives with the connection between donor and acceptor, defining the dihedral angle $\measuredangle_{DA}$ highlighted in blue. Hole (h^+) and electron (e^-) natural transition orbitals for the $D_0 \rightarrow D_1$ transition in b) TBTM, and c) TTM, both functionalized with TPA, 3PCz, and PCz electron donors in their ground state geometries, calculated using CAM-B3LYP, ($\gamma = 0.098\ a_0^{-1}$) def2-SVP.

the hole NTO remains on the donor unit. However, for the TBTM radical series, we observe a much more stringent charge separation, whereas the TTM series is characterized by substantial overlap between electron and hole NTOs, rendering the transition state more hybridized with contribution from a locally excited and a charge transfer state (HLCT).[3,8,25] These observations align well with our experimental results, corroborating the stronger CT character for the TBTM radicals and the HLCT behavior for the TTM series. The spectra of the TTM radicals show a series of absorption events between 400 and 500 nm in addition to the above-discussed bands, which are absent in TBTM (see Figure 2). These bands result from transitions to higher-lying excited states with significantly smaller oscillator strength in the TBTM compared to the TTM series. The diminished transition probability is reasonable when considering that the higher-lying excited states will involve orbitals on both donor and acceptor moieties, which will be more decoupled for the TBTM radicals with the more perpendicular donor to trityl planes. Thus, the UV–vis spectra of the TBTM series consist only of the features of the isolated donor and acceptor species, apart from the $D_0 \rightarrow D_1$ transition (see Figure 2).

2.3. Character of the Excited State and the Transitions to the Ground State

When we compare the photoluminescence spectra of the TBTM derivatives to the TTM series, we observe that the spectra are less structured for the TBTM than for TTM, while the spectra are equally broad (see Figure 2). Presumably, coupling to vibrational modes appears with higher disorder and the lifetimes of the modes are shorter resulting in broadening of the signal. The emission of TBTM-PCz and TBTM-3PCz is blueshifted compared to their TTM homologues. This altered excited state behavior of the TBTM derivatives comes with lower photostability when compared to the TTM analogs (see Figures S25–S27, Supporting Information). The light-induced ring-closing reaction known to be the reason for the poor stability of some trityl derivatives toward UV light appears to be facilitated through the additional chlorines.[26,27]

We determine ϕ_{PL} of the donor-functionalized TBTM and TTM radicals in cyclohexane (see Table 1). ϕ_{PL} is drastically increased for the donor-functionalized TBTM radicals compared to the TTM series, with a maximum ϕ_{PL} of 59% for TBTM-3PCz (see Table 1). We have previously shown that the donor strength of the substituent needs to be adjusted to the electron-accepting capability of the radical moiety to ensure maximum emission efficiency by suppression of non-radiative decay pathways.[12] TBTM will be a slightly stronger acceptor than TTM for the larger number of electron-withdrawing chlorine atoms. Therefore, the increase in ϕ_{PL} could also be an effect of the more balanced donor-acceptor combination. In other words, 3PCz is a suitable donor for TBTM, while it might have slightly too low electron-donating capability for TTM, representing a weaker acceptor, which results in a less pronounced charge separation in the excited state. Additionally, the electronic properties of the whole molecule are determined by the interplay of donor and acceptor. This becomes evident from the oxidation potentials for the donors being modified by attachment to the different trityls as observed in the cyclic voltammograms (see Figure S24, Supporting Information). Apart from adjusting the donor strength, the CT character of the excited state can also be tuned by the solvent polarity. More polar solvents are expected to stabilize the CT state and favor intramolecular charge migration. Indeed, we find ϕ_{PL} of TBTM-PCz to be increased from 16 to 34%, when changing the solvent to slightly more polar toluene. By contrast, TBTM-TPA and TTM-TPA exhibit identical emission maxima λ_{em} of 729 nm, whereas the ϕ_{PL} value is greatly increased for TBTM-TPA (43%) versus TTM-TPA (12%) (see Table 1). Therefore, we hypothesize that the increase in ϕ_{PL} is related to the reduced LE character and restricted rotation around the bond between donor and trityl acceptor.

2.4. Time-Resolved Spectroscopy

To elucidate the reasons for the improved emission performance of the donor-functionalized TBTM radicals versus the TTM derivatives, we probe our molecules by transient absorption (TA) spectroscopy. We take a closer look at the TPA-donor functionalized trityl radicals, since both types of TTM and TBTM radicals delivered similar emission spectra, despite the much greater ϕ_{PL} in the TBTM-TPA derivative (cf.Figures 2 and 4 and Table 1). The TA spectra for the other PCz and 3PCz functionalized TBTM and TTM radicals exhibit the same qualitative effects and are therefore shown in the Supporting Information in Figures S14–S19 (Supporting Information).

The dynamics of the photoexcited state populations in the TTM and TBTM derivatives are investigated in cyclohexane solution by excitation to the D1 state by pumping at λ_{ex} = 630 nm for the TPA derivatives (and λex = 550 nm for the PCz and 3PCz derivatives), as well as into a higher locally excited state by pumping at λ_{ex} = 375 nm, resonant with the observed UV–vis maxima (cf. Figures 2,4) (see section S4, Supporting Information for a detailed experimental description). TTM-TPA shows one strong excited state absorption (ESA) band between 600–900 nm, split into a double peak by the stimulated emission around 720 nm (see **Figure 5a**). This ESA transition can be assigned to the $D_1 \rightarrow D_2$ excitation.[28] A secondary ESA feature is observed at 1600 nm (see Figure 4a). For TBTM-TPA, three bands with enhanced intensities appear (see Figure 4c). As for TTM, the band between 600–750 nm is assigned to the $D_1 \rightarrow D_2$ excitation. The two new bands at 460 and 800 nm are assigned to the TBTM anion and triphenylamine radical cation, respectively, of the CT state, based on reported spectro-electrochemical TA spectroscopy of triarylamine-donor functionalized trityl radicals.[20,29,30] The observation of these two separate bands indicates strong electronic decoupling of the donor and acceptor unit, corroborating their close-to-perpendicular orientation, which is in agreement with our computed ground and excited state geometries. A further excited state absorption band appearing at 1100 nm is likely related to this enhanced CT character. Similar to TBTM-TPA, new bands appear for the PCz- and 3PCz-substituted TBTMs at 450 and 850 nm (see Figures S17,S19, Supporting Information). The lowest increase in ϕ_{PL} for the TBTM-derivative of the 3PCz-donor is reflected in the much less pronounced CT-ESA signals (see Figure S17, Supporting Information compared to the TPA- and PCz- donor). A more in-detail investigation of the difference between the donor-moieties would be of interest, but the low

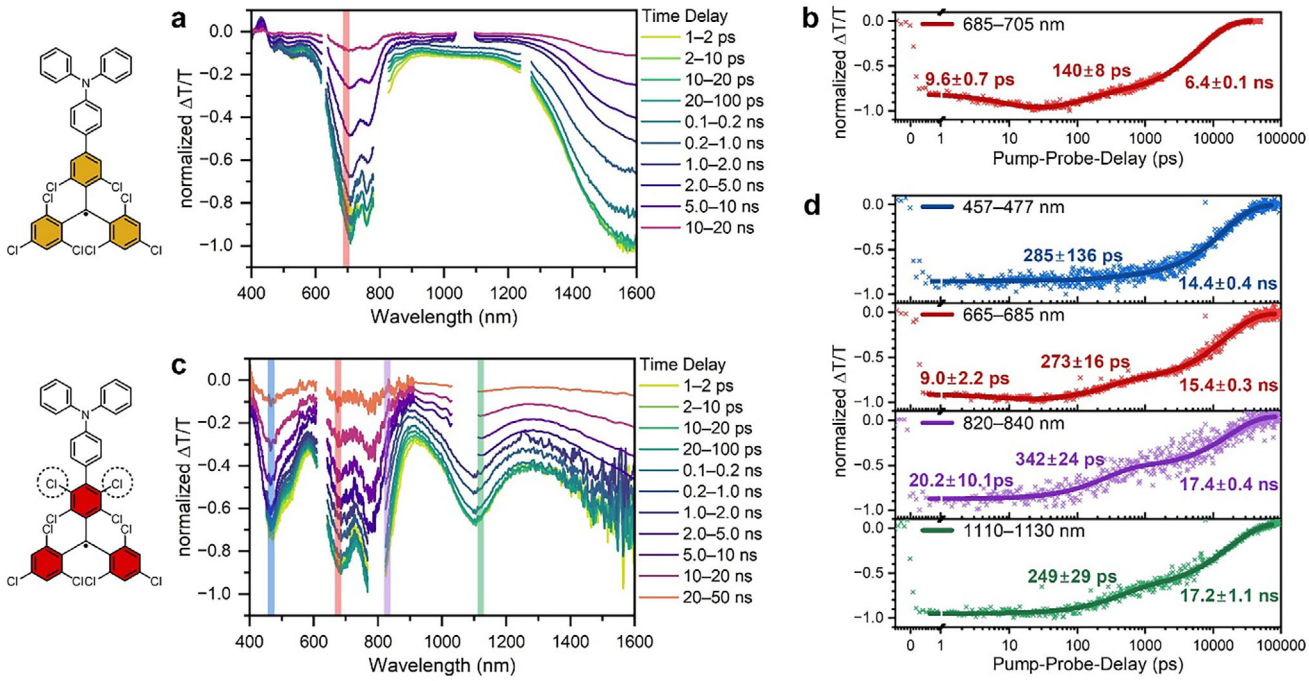

Figure 4. Normalized transient absorption spectra at time delays as indicated a,c) and kinetic traces b,d) of compounds TTM-TPA and TTBM-TPA dissolved in cyclohexane upon excitation at 630 nm. Gaps in the spectra are due to the laser fundamentals.

photostability of the 3PCz-functionalized TBTM derivatives limits the gained insights. The effect of donor-strength on the CT-state and thereby the emission characteristics of TTM-Donor radicals has been further investigated in prior work.[12]

The ESA features of both TTM-TPA and TBTM-TPA show a similar rise time after excitation (within our time resolution). By contrast, the decay times are extended for the TBTM-derivative (cf. Figure 4b,d). Their longest excited state lifetimes, as determined using biexponential fits to the TA spectroscopy data (6.4 ns for TTM-TPA and 14.4–17.4 ns for TBTM-TPA), match the photoluminescence lifetimes τ determined by transient photoluminescence spectroscopy (6.4 ns for TTM-TPA and 17.1 ns for TBTM-TPA) (cf. Figure 4b,d with Table 1 and Figure S20, Supporting Information). Both spectroscopic techniques confirm that the excited D_1 state decays much faster in TTM-TPA than in TBTM-TPA. The increased excited state lifetime in TBTM-TPA combined with the higher ϕ_{PL} indicates that there are fewer non-radiative decay pathways, compared to the TTM-TPA radical. The TA spectra of the other donor functionalized radicals lead to the same conclusion (see Figure S16–S19, Supporting Information).

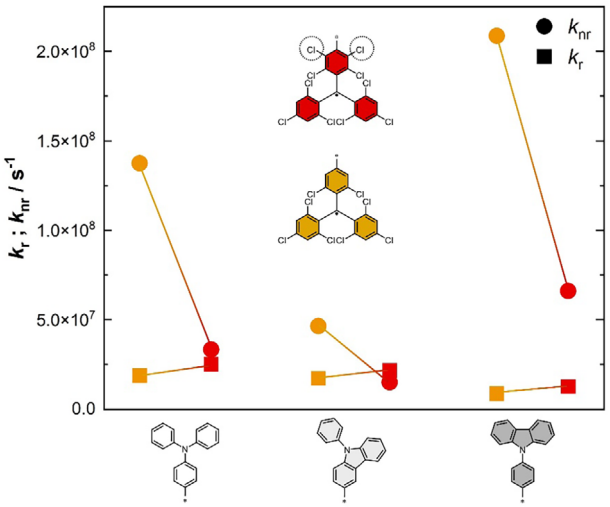

Figure 5. Rate constants of radiative (squares) and non-radiative (circles) relaxation for the different donor-functionalized radicals.

After excitation with the λ_{ex} = 375 nm laser into higher excited states (D_2 and higher), the TA spectra show a population increase of the D1 state over the course of the first 100 ps, due to relaxation from these higher excited states (see b panels in Figures S14–S19, Supporting Information)a population increase of the D_1 state over the course of the first 100 ps, due to relaxation from these higher excited states These observed relaxation kinetics for donor-functionalized TBTM and TTM radicals are on similar timescales consistent with internal conversion.

We use the determined lifetimes τ of the D_1 state to determine the rate constants for radiative (k_r) and non-radiative (k_{nr}) relaxation (see Table 1) using the following well-known relations:

$$\phi_{PL} = \frac{k_r}{k_r + k_{nr}} \quad (1)$$

$$\tau = \frac{1}{k_r + k_{nr}} \quad (2)$$

Altogether, k_r is of the same order of magnitude for all radicals (see Figure 5). A slight increase of k_r is observed for all electron donors when exchanging the TTM unit for TBTM. By contrast, k_{nr} varies greatly and appears strongly reduced for the donor functionalized TBTM radicals compared to the TTM radical series. Therefore, k_{nr} appears to be the main descriptor of ϕ_{PL}. For all three TBTM radicals, we find much smaller k_{nr} as compared to the TTM series (see Figure 5).

2.5. Huang Rhys Factors

To elucidate the reasons for the suppression of non-radiative decay in the TBTM series, we theoretically investigate the coupling of the excited state to vibrational modes. To gain insight into the level of steric hindrance of the rotation of the donor moieties against the trityl plane, we compute the Huang–Rhys (HR) factors for the $D_0 \rightarrow D_1$ transition in the lower energy frequency domain, representing the torsional modes.[31] In the TTM series, we observe strong HR factors for frequencies $\approx$210 cm^{-1}, typical for torsional modes (see Figures S9,S10, Supporting Information for illustration of the modes). Interestingly, these HR factors are significantly weakened in the donor-functionalized TBTM series, confirming that the additional chlorine atoms indeed provide sufficient steric hindrance to inhibit the torsional modes of the donor against the trityl plane (cf. Figure 3 with Figures S9,S10, Supporting Information).

To obtain a mechanistic understanding of our systems, we apply a semi-quantitative analysis based on the expression.

$$k_{m\rightarrow n} = \frac{\pi}{\hbar}\left(\sum_{\mu}\left|D_{\mu}^{(mn)}\right|^2\right)\sum_{(\nu_\mu)}\left(\prod_{\mu}\frac{\left(S_{\mu}^{(mn)}\right)^{\nu_\mu}}{\nu_\mu!}e^{-S_{\mu}^{(mn)}}\right)\delta \left(E_m - E_n - \sum_{\mu}\nu_\mu\hbar\omega_\mu\right) \quad (3)$$

of the rate constant for non-radiative decay.[32,33] The first summation in Equation (3) contains the projection $D_{\mu}^{(mn)}$ of the nonadiabatic coupling vector between the electronic states m and n on the normal mode μ:

$$D_{\mu}^{(mn)} = \hbar\omega_\mu \langle\psi_m| \frac{\partial}{\partial Q_\mu} |\psi_n\rangle\Big|_{Q_\mu=0} \quad (4)$$

where ω_μ and Q_μ are the angular frequency and normal coordinate, respectively, of the mode μ, and ψ_m and ψ_n the electronic wave functions of the two involved states. The second summation in Equation (3) runs over the set of all possible combinations of vibrational quanta (ν_μ) among the modes μ and can be recognized as the energy-shifted and Franck–Condon weighted density of states (FCWD). The Franck–Condon factors are expressed by HR factors $S_{\mu}^{(mn)}$, E_m and E_n are the adiabatic energy of the electronic states and $\delta(\cdot)$ the Dirac delta function that ensures energy conservation.[33] The HR factors represent a measure for exciton-phonon coupling. In section S3.4 (Supporting Information), we give a more detailed account of the HR factor and its influence on the rate constant $k_{m\rightarrow n}$, and discuss the assumptions involved in our approach. Here, we stress that the HR factors determine the FCWD and that HR factors related to high-frequency modes are considered to promote fast non-radiative decay.[18,34] Therefore, we can obtain a semi-quantitative understanding of the non-radiative decay in our systems by considering nonadiabatic and exciton-phonon coupling for the first excited state.

When calculating the HR factors for the $D_0 \rightarrow D_1$ transition in the high-frequency range from 1000 to 1700 cm^{-1}, we observe only weak vibrational coupling to the exciton for both, the donor-functionalized TTM and the TBTM radicals (see Figure S11, Supporting Information). The strongest mode close to 1600 cm^{-1} is present in all TTM-based radicals and has previously been detected in computational Huang–Rhys factor analysis and experimentally by excited state vibrational spectroscopy in TTM-TPA.[18,20] This mode has been identified as a C-C and C-H breathing mode of the phenyl rings in the trityl moiety.[15,18] The breathing mode can couple to the exciton and cause non-radiative decay. Beneficially for high values of ϕ_{PL}, this mode is suppressed in our TBTM radical series (see Figure S11, Supporting Information). However, the HR factors are generally too small to explain the pronounced difference of the ϕ_{PL} values of the different series.

Donor-acceptor systems based on a functionalized trityl moiety can exhibit electronic-state hybridization between the D_1 state and the D_2 state, where the D_1 state typically bears CT character and the D_2 state is a dark LE state.[25,35] If hybridization becomes relevant, the expression for $k_{1\rightarrow 0}$ in Equation (1) needs to be extended beyond the two-state model as to include contributions from the D_2 state (see Figure S13, Supporting Information for $D_0 \rightarrow D_2$ NTOs and section S3.2, Supporting Information for details). In our analysis, we account for these potential contributions by also considering the nonadiabatic coupling vector between the first two excited states and the HR factors related to the D_2 state. Please note that our semi-quantitative approach mainly allows for the comparison between a TBTM system and its TTM analog and thus for an understanding of the alteration of non-radiative decay upon additional chlorination.

We can understand the non-radiative decay in our systems in terms of the nonadiabatic coupling vectors $D^{(mn)}$ between the electronic states m and n, and the HR factors S_μ. The norms of the coupling vectors $D^{(01)}$ and $D^{(12)}$ for the TTM and TBTM series are listed in Table 1. It becomes obvious that in every case the coupling between the D_1 and D_2 state is considerably larger than the coupling between the D_1 state and the ground state D_0. This implies an electronic hybridization between the first two excited states in all systems. Thus, the exciton-phonon coupling in the D_2 state influences the non-radiative decay of the D_1 state. For TBTM-PCz and TBTM-TPA, the norms for $D^{(01)}$ and $D^{(12)}$ are consistently smaller than for the TTM analogs. This is in accordance with the clear CT observed in the TA spectra. The diminished CT-LE hybridization suppresses non-radiative relaxation, which agrees well with the experimentally observed trend of improved ϕ_{PL} for the TBTM series. Qualitatively, the reduced nonadiabatic couplings can be understood in terms of the Mulliken–Hush approach, where the coupling between two electronic states is approximately inversely proportional to the change in molecular dipole moment.[36] Hence, the decreased coupling for TBTM-PCz and TBTM-TPA can be linked to the marked CT character in the D_1 state. Obviously, the close-to-perpendicular orientation

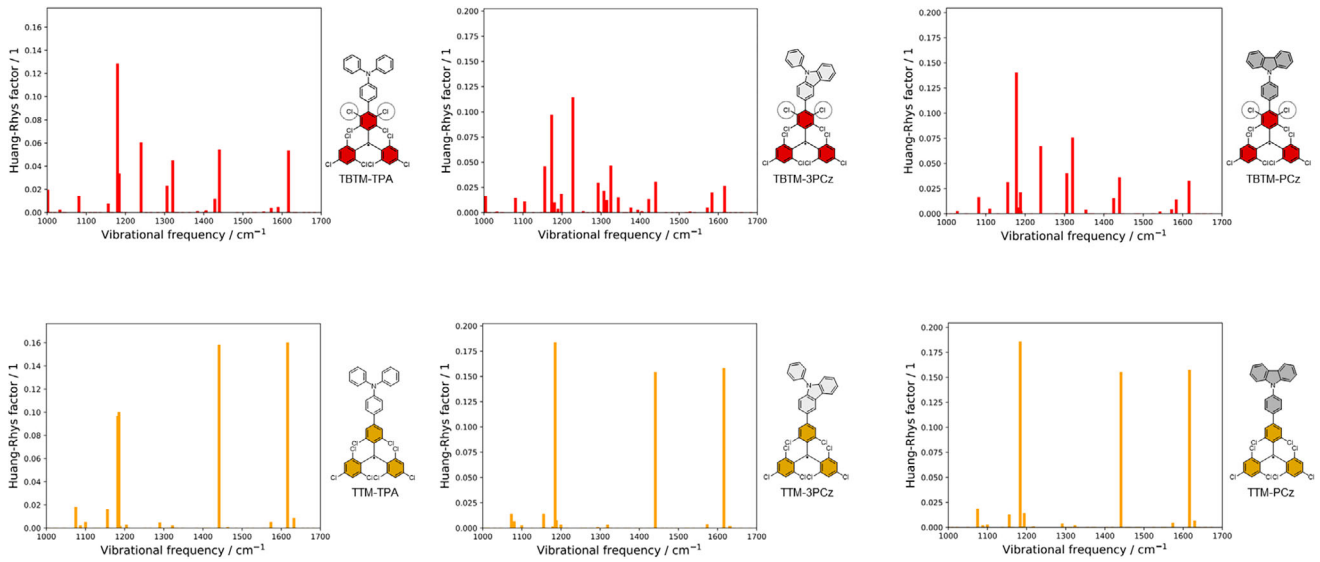

Figure 6. Huang–Rhys factors for the D_2 states in the high-frequency domain as a measure for exciton-phonon coupling (TBTM: red, TTM: orange). Due to considerable electronic hybridization between the D_1 and D_2 states, the HR factors in the D_2 state influence non-radiative decay. Calculations performed on the CAM-B3LYP/def2-SVP level of theory.

of donor and acceptor units in the TBTM series induces pronounced charge-separation and thus hinders the hybridization of CT and LE states due to a lack of orbital overlap.

In contrast to the other two TBTM derivatives, for TBTM-3PCz we observe a pronounced coupling between the D_1 and D_2 state, which is even increased with respect to the TTM analog (see Table 1). Despite this strong coupling, which is considered to favor non-radiative decay, TBTM-3PCz still shows improved ϕ_{PL} when compared to TTM-3PCz. This experimental observation can be rationalized by the altered exciton-phonon coupling of the D_2 state. For the case of significant CT-LE hybridization, the HR factors of this state give insights into non-radiative relaxation. For the TTM series, we observe three vibrational modes in the higher frequency domain that strongly couple to the D_2 excited state (see **Figure 6**). By contrast, in the TBTM series, the HR factors of these modes are diminished.

The modes around ≈1185 cm^{-1} partly extend to the donor fragment, whereas the other two modes are primarily confined to the TTM moiety (see Figure S12, Supporting Information). Especially in the frequency region of these two modes, exciton-phonon coupling of the TBTM systems is either suppressed or absent. This behavior can be explained by recalling the enhanced CT character of the D_1 state in all TBTM systems. It follows that the spatial separation between hole and particle orbitals for the transition between D_0 and D_1 state is increased, which is shown to suppress non-radiative deactivation pathways.[18] Therefore, we can understand the improved non-radiative rate constants of TBTM-PCz and TBTM-TPA by a combined effect of reduced nonadiabatic coupling and suppressed exciton-phonon coupling in the D_2 state. For TBTM-3PCz, ϕ_{PL} is improved compared to TTM-3PCz despite the comparatively strong nonadiabatic coupling between the D_1 and D_2 states. The decreased coupling to high-frequency modes in both the D_1 and D_2 excited states allows for the efficient suppression of non-radiative relaxation.

3. Conclusion

We have introduced a new series of donor-functionalized radicals by employing a TTM radical with two additional chlorine atoms in *meta*-position to the methinyl radical carbon. The additional chlorines apply steric constraints on the rotational freedom of the doner against the trityl radical acceptor. The donor and trityl moiety are forced into a close-to-perpendicular orientation, leading to a pronounced charge separation in the excited state. We find highly improved values of ϕ_{PL} compared to the TTM reference series functionalized with identical donors by suppressing nonradiative decay pathways. Our molecular design approach presents a new strategy in light-emitting radicals to tune the optical properties, such as decay rates and ϕ_{PL}. In the future, this approach will allow the design and synthesis of highly efficient light-emitting radicals with redshifted emission into the near IR that could overcome the limits and restrictions imposed by the energy gap law.

Supporting Information

Supporting Information is available from the Wiley Online Library or from the author.

Acknowledgements

M.E.A, R.T., and L.S. contributed equally to this work. The authors acknowledge support by the state of Baden-Württemberg through bwHPC and the German Research Foundation (DFG) through grant no INST 40/575-1 FUGG (JUSTUS 2 cluster). We acknowledge funding by the Deutsche Forschungsgemeinschaft (DFG, German Research Foundation) under project numbers: 500226157, 445471845, 445471097, 445470598. Mona E. Arnold, Robert Toews, and Lars Schneider contributed equally to this work.

Open access funding enabled and organized by Projekt DEAL.

Conflict of Interest

The authors declare no conflict of interest.

Data Availability Statement

The data that support the findings of this study are available in the supplementary material of this article.

Keywords

DFT, light emitting radicals, transient absorption spectroscopy, triaryl methyl radicals, TTM

Received: February 25, 2025
Revised: March 28, 2025
Published online: April 21, 2025

[1] J. Ding, S. Dong, M. Zhang, F. Li, *J Mater Chem C Mater* **2022**, *10*, 14116.
[2] J. M. Hudson, T. J. H. Hele, E. W. Evans, *J. Appl. Phys.* **2021**, *129*, 180901.
[3] C. He, Z. Li, Y. Lei, W. Zou, B. Suo, *J. Phys. Chem. Lett.* **2019**, *10*, 574.
[4] A. Abdurahman, T. J. H. Hele, Q. Gu, J. Zhang, Q. Peng, M. Zhang, R. H. Friend, F. Li, E. W. Evans, *Nat. Mater.* **2020**, *19*, 1224.
[5] H. H. Cho, S. Gorgon, G. Londi, S. Giannini, C. Cho, P. Ghosh, C. Tonnelé, D. Casanova, Y. Olivier, T. K. Baikie, F. Li, D. Beljonne, N. C. Greenham, R. H. Friend, E. W. Evans, *Nat. Photonics* **2024**, *18*, 905.
[6] Q. Peng, A. Obolda, M. Zhang, F. Li, *Angew. Chem., Int. Ed.* **2015**, *54*, 7091.
[7] V. Gamero, D. Velasco, S. Latorre, F. López-Calahorra, E. Brillas, L. Juliá, *Tetrahedron Lett.* **2006**, *47*, 2305.
[8] L. Fajarí, R. Papoular, M. Reig, E. Brillas, J. L. Jorda, O. Vallcorba, J. Rius, D. Velasco, L. Juliá, *J. Org. Chem.* **2014**, *79*, 1771.
[9] L. Chen, M. Arnold, Y. Kittel, R. Blinder, F. Jelezko, A. J. C. Kuehne, *Adv. Opt. Mater.* **2022**, *10*, 2102101.
[10] P. Murto, B. Li, Y. Fu, L. E. Walker, L. Brown, A. D. Bond, W. Zeng, R. Chowdhury, H. H. Cho, C. P. Yu, C. P. Grey, R. H. Friend, H. Bronstein, *J. Am. Chem. Soc.* **2024**, *146*, 13133.
[11] K. Nakamura, K. Matsuda, R. Xiaotian, M. Furukori, S. Miyata, T. Hosokai, K. Anraku, K. Nakao, K. Albrecht, *Faraday Discuss.* **2023**, *250*, 192.
[12] M. E. Arnold, L. Roß, P. Thielert, F. Bartley, J. Zolg, F. Bartsch, L. A. Kibler, S. Richert, C. Bannwarth, A. J. C. Kuehne, *Adv. Opt. Mater.* **2024**, *12*, 2400697.
[13] S. Dong, W. Xu, H. Guo, W. Yan, M. Zhang, F. Li, *Phys. Chem. Chem. Phys.* **2018**, *20*, 18657.
[14] Z. Li, J. Wang, X. Liu, P. Gao, G. Li, G. He, B. Rao, *Angew. Chem., Int. Ed.* **2023**, *62*, 2302835.
[15] C. Lu, E. Cho, K. Wan, C. Wu, Y. Gao, V. Coropceanu, J. L. Brédas, F. Li, *Adv. Funct. Mater.* **2024**, *34*, 2314811.
[16] C. Wu, C. Lu, S. Yu, M. Zhang, H. Zhang, M. Zhang, F. Li, *Angew. Chem., Int. Ed.* **2024**, *63*, 2412483.
[17] Y. Hattori, R. Kitajima, W. Ota, R. Matsuoka, T. Kusamoto, T. Sato, K. Uchida, *Chem. Sci.* **2022**, *13*, 13418.
[18] P. Ghosh, A. M. Alvertis, R. Chowdhury, P. Murto, A. J. Gillett, S. Dong, A. J. Sneyd, H. H. Cho, E. W. Evans, B. Monserrat, F. Li, C. Schnedermann, H. Bronstein, R. H. Friend, A. Rao, *Nature* **2024**, *629*, 355.
[19] C. Lu, E. Cho, Z. Cui, Y. Gao, W. Cao, J. L. Brédas, V. Coropceanu, F. Li, *Adv. Mater.* **2023**, *35*, 2208190.
[20] A. Heckmann, S. Dümmler, J. Pauli, M. Margraf, J. Köhler, D. Stich, C. Lambert, I. Fischer, U. Resch-Genger, *J. Phys. Chem. C* **2009**, *113*, 20958.
[21] M. E. Arnold, A. J. C. Kuehne, *Dyes Pigm.* **2023**, *208*, 110863.
[22] K. Matsuda, R. Xiaotian, K. Nakamura, M. Furukori, T. Hosokai, K. Anraku, K. Nakao, K. Albrecht, *Chem. Commun.* **2022**, *58*, 13443.
[23] T. Yanai, D. P. Tew, N. C. Handy, *Chem. Phys. Lett.* **2004**, *393*, 51.
[24] F. Weigend, R. Ahlrichs, *Phys. Chem. Chem. Phys.* **2005**, *7*, 3297.
[25] E. Cho, V. Coropceanu, J. L. Brédas, *J. Am. Chem. Soc.* **2020**, *142*, 17782.
[26] M. A. Fox, E. Gaillard, C.-C. Chen, *J. Am. Chem. Soc.* **1987**, *109*, 7088.
[27] S. R. Ruberu, M. A. Fox, *J. Phys. Chem.* **1993**, *97*, 143.
[28] X. Ai, E. W. Evans, S. Dong, A. J. Gillett, H. Guo, Y. Chen, T. J. H. Hele, R. H. Friend, F. Li, *Nature* **2018**, *563*, 536.
[29] R. Maksimenka, M. Margraf, J. Köhler, A. Heckmann, C. Lambert, I. Fischer, *Chem. Phys.* **2008**, *347*, 436.
[30] H. Guo, Q. Peng, X. K. Chen, Q. Gu, S. Dong, E. W. Evans, A. J. Gillett, X. Ai, M. Zhang, D. Credgington, V. Coropceanu, R. H. Friend, J. L. Brédas, F. Li, *Nat. Mater.* **2019**, *18*, 977.
[31] K. Huang, A. Rhys, *Proc. R. Soc. A* **1950**, *204*, 406.
[32] A. S. Bozzi, W. R. Rocha, *J. Chem. Theory Comput.* **2023**, *19*, 2316.
[33] L. Shi, X. Xie, A. Troisi, *J. Chem. Phys.* **2022**, *157*, 134106.
[34] J. S. Wilson, N. Chawdhury, M. R. A. Al-Mandhary, M. Younus, M. S. Khan, P. R. Raithby, A. Köhler, R. H. Friend, *J. Am. Chem. Soc.* **2001**, *123*, 9412.
[35] E. Cho, V. Coropceanu, J. L. Brédas, *J Mater Chem C Mater* **2021**, *9*, 10794.
[36] R. J. Cave, M. D. Newton, *Chem. Phys. Lett.* **1996**, *249*, 15.